

# Model-independent $H_0$ within FLRW: Joint constraints from GWTC-3 standard sirens and strong lensing time delays

Ji-Yu Song,<sup>1</sup> Jing-Zhao Qi,<sup>1,\*</sup> Jing-Fei Zhang,<sup>1</sup> and Xin Zhang<sup>1, 2, 3, †</sup>

<sup>1</sup>*Key Laboratory of Cosmology and Astrophysics (Liaoning Province) & Department of Physics, College of Sciences, Northeastern University, Shenyang 110819, China*

<sup>2</sup>*Key Laboratory of Data Analytics and Optimization for Smart Industry (Ministry of Education), Northeastern University, Shenyang 110819, China*

<sup>3</sup>*National Frontiers Science Center for Industrial Intelligence and Systems Optimization, Northeastern University, Shenyang 110819, China*

The Hubble tension has emerged as a critical crisis in cosmology, with the cause remaining unclear. Determining the Hubble constant ( $H_0$ ) independently of cosmological models and distance ladders will help resolve this crisis. In this letter, we for the first time use 47 gravitational-wave (GW) standard sirens from the third Gravitational-Wave Transient Catalog to calibrate distances in the strong lensing system, RXJ1131-1231, and constrain  $H_0$  through the distance-sum rule, with minimal cosmological assumptions. We assume that light propagation over long distances is described by the Friedmann-Lemaître-Robertson-Walker metric and that geometrical optics holds, but we do not need to assume the universe's contents or the theory of gravity on cosmological scales. Fixing  $\Omega_K = 0$ , we obtain  $H_0 = 73.22^{+5.95}_{-5.43} \text{ km s}^{-1} \text{ Mpc}^{-1}$  and  $H_0 = 70.40^{+8.03}_{-5.60} \text{ km s}^{-1} \text{ Mpc}^{-1}$  by using the deflector galaxy's mass model and kinematic measurements to break mass-sheet transform, respectively. When  $\Omega_K$  is not fixed, the central value of  $H_0$  increases further. We find that our results are still dominated by statistical errors, and at the same time, we notice the great potential of using GW dark sirens to provide calibration, owing to their higher redshifts. When using 42 binary black holes and RXJ1131-1231, we obtain a 8.46%  $H_0$  constraint precision, which is better than that from the bright siren GW170817 using the Hubble law by about 40%. In the future, as the redshift range of GW dark sirens increases, more and more SGLTDs can be included, and we can achieve high-precision, model-independent measurements of  $H_0$  without the need for GW bright sirens.

*Introduction.*— The six-parameter  $\Lambda$  cold dark matter ( $\Lambda$ CDM) model is successful, which can explain most cosmic observations and fit the cosmic microwave background (CMB) data with stunning precisions. However, the tensions in some parameter measurements from different observations challenge the internal consistency of the  $\Lambda$ CDM model, especially the Hubble tension. The Hubble constant ( $H_0$ ) inferred by globally fitting the  $\Lambda$ CDM model to the Planck CMB measurements is in over  $5\sigma$  tension with that measured with the SH0ES (Supernovae and  $H_0$  for the Equation of State of dark energy) distance ladder [1, 2]. Determination of the cause of the Hubble tension is significant, as it could hint at the new physics beyond the  $\Lambda$ CDM model. Currently, no extended cosmological model can resolve the Hubble tension and agree well with observations at the same time [3–5], while numerous studies demonstrated that systematics in observations may not explain the serious discrepancy of  $H_0$  [2, 6–10], including using the high-precision James Webb Space Telescope [11–15]. However,  $H_0$  values from distance ladders using different calibrators and distance indicators are inconsistent [16, 17], pushing continuous efforts to search for potential systematical bias in SH0ES measurements [18–20]. In summary, research and discussion on the Hubble tension is still going on. A cosmological-model-independent measurement of  $H_0$  from the third-party observations undoubtedly helps resolve the Hubble tension.

Recently, based on the distance sum rule in the Friedmann-Lemaître-Robertson-Walker (FLRW) metric [21], Ref. [22] used Type Ia supernovae (SNe Ia) and the strong gravitational lensing time delays (SGLTDs) to measure  $H_0$  and  $\Omega_K$  without assuming a specific cosmological model. In an SGLTD system, the time delay relates to the time-delay distance, and the time-delay distance is a ratio of three angular distances (the observer to the deflector galaxy, the observer to the source, and the deflector galaxy to the source). In the FLRW metric, these three distances are interconnected via the distance sum rule, incorporating  $H_0$  and  $\Omega_K$ . Consequently, using SNe Ia as standard candles to calibrate these three distances, one can constrain  $H_0$  and  $\Omega_K$  without reliance on specific cosmological models. However, the uncalibrated SNe Ia cannot measure the absolute luminosity distances but the relative distances, so when using the uncalibrated SNe Ia in this method, SNe Ia's absolute magnitude  $M_B$  is entirely degenerate with  $H_0$ , which is theoretically problematic as without any observations to constrain  $M_B$ . After that, Ref. [23] used the ultraviolet versus X-ray luminosity correlation of quasars to calibrate distances in SGLTD systems and measured  $H_0$  and  $\Omega_K$ . Ref. [24] made a forecast using strongly lensed SNe Ia in this method.

Gravitational-wave (GW) standard sirens can provide self-calibrated luminosity distance measurements and are the better distance indicator. GWs from compact binary

coalescences encode luminosity distances directly in their waveform amplitudes, and when obtaining redshifts of GW sources, it is possible to constrain the cosmic expansion history [25]. Detecting the electromagnetic (EM) counterpart of the GW source can help identify the GW source's host galaxy and determine the redshift [25–28]. Depending on whether an EM counterpart is detected, GW standard sirens are categorized into “bright sirens” [29–41] and “dark sirens” [42–52]. Recently, Ref. [53] proposed using GW bright sirens to calibrate distances in SGLTDs and constrain  $H_0$  and  $\Omega_K$ . Since there is only one bright siren, GW170817 [26], being observed, they implemented their method on mock data.

In this letter, we extend the method of Ref. [53] by considering the use of GW dark sirens. GW bright sirens, which are binary neutron stars (BNSs) and neutron star-black holes (NSBHs) with EM counterpart detections, have limited detection ranges. In contrast, GW dark sirens' main sources are binary black holes (BBHs), which have larger masses and wider detection ranges. Furthermore, we can obtain GW dark sirens' redshifts using source-frame mass distribution models of GW sources and galaxy catalogs. Therefore, using GW dark sirens, we can extend the redshift range of GW data to calibrate more SGLTDs. For the first time, we can use real observed GW data and SGLTD data to measure  $H_0$  without assuming a specific cosmological model.

*Methodology.—The distance sum rule.* If space is homogeneous and isotropic, spacetime is described by the FLRW metric. Under the assumption that geometrical optics holds and the time-redshift relation  $t(z)$  is monotonic, the angular diameter distance  $D_A(z_d, z_s)$  between a defector galaxy at redshift  $z_d$  and a source at redshift  $z_s$  can be expressed in terms of the dimensionless distance  $d(z_d, z_s) = (1 + z_s)H_0D_A(z_d, z_s)$ , defined as:

$$d(z_d, z_s) = \frac{1}{\sqrt{|\Omega_K|}} \text{sinn}(\sqrt{|\Omega_K|} \int_{z_d}^{z_s} \frac{H_0}{H(z)} dz), \quad (1)$$

where

$$\text{sinn}(x) = \begin{cases} \sin(x), & \Omega_K < 0, \\ x, & \Omega_K = 0, \\ \sinh(x), & \Omega_K > 0. \end{cases}$$

Here,  $H(z)$  is the Hubble parameter, and  $\Omega_K = -K/H_0^2$ .  $K$  is a constant describing the spatial curvature. For simplicity, we define  $d_d \equiv d(0, z_d)$ ,  $d_s \equiv d(0, z_s)$ , and  $d_{ds} \equiv d(z_d, z_s)$ , and these three dimensionless distances are connected via the distance sum rule [21]

$$\frac{d_{ds}}{d_s} = \sqrt{1 + \Omega_K d_d^2} - \frac{d_d}{d_s} \sqrt{1 + \Omega_K d_s^2}, \quad (2)$$

which can be further written as

$$\frac{d_d d_s}{d_{ds}} = \frac{1}{\sqrt{1/d_d^2 + \Omega_K} - \sqrt{1/d_s^2 + \Omega_K}}. \quad (3)$$

*Time delay and distances.* In an SGLTD system, the arrival time delay  $\Delta t_{ij}$  between two images at  $\theta_i$  and  $\theta_j$  is given by [54, 55]

$$\Delta t_{ij} = D_{\Delta t} \Delta \phi_{i,j} = \frac{1}{H_0} \frac{d_d d_s}{d_{ds}} \Delta \phi_{ij}, \quad (4)$$

where  $D_{\Delta t}$  is the time-delay distance, and  $\Delta \phi_{ij}$  is the Fermat potential difference of these two images. Given  $\Delta t_{ij}$ ,  $d_d$ ,  $d_s$ , and an inference of  $\Delta \phi_{ij}$ , we can determine  $H_0$  and  $\Omega_K$  from Eqs. (3) and (4) without relying on a specific cosmological model.

*Obtaining redshifts for GW standard sirens.* Detections of EM counterparts can help localize GW sources' host galaxies, thus determining redshifts [25–28]. We adopt two methods to obtain redshifts for GW standard sirens without EM counterparts. The first method uses the population model of GW sources, called the spectral siren method [56, 57]. The waveform phase of the GW standard siren determines the redshifted masses  $m_{1,z}$  and  $m_{2,z}$ , which are related to the source-frame masses  $m_1$  and  $m_2$  via

$$m_i = \frac{m_{i,z}}{1+z}. \quad (5)$$

We can break the degeneracy between mass and redshift by modeling the mass and redshift distributions in the source frame, hence extracting redshift. This method is more efficient when the mass distribution has sharp features [57].

The second method involves searching for potential host galaxies of GW sources using a galaxy catalog, known as the dark siren approach [25, 58, 59]. The GW observation provides a rough localization region of the GW source, and the galaxy catalog provides redshifts of galaxies in this region, which may include the host galaxies of the GW source. Assuming the probability of a galaxy being the host is related to its luminosity, the galaxies in the localization region of the GW source give a roughly redshift distribution for the GW source. Due to the limited observational capability of survey telescopes, the completeness of the galaxy catalog decreases with distance. In the incomplete part, the redshift information is from the redshift prior of GW sources, i.e., from the spectral siren method.

*Observations.—Gravitational wave data.* We use 47 GW standard sirens with a signal-to-noise ratio greater than 11 and an inverse false alarm rate greater than 4 yr from the third Gravitational-Wave Transient Catalog (GWTC-3), roughly covering the redshift range of  $z < 0.8$ . These include 42 BBHs, three NSBHs, and two BNSs.

We obtain the redshift of GW170817 from its EM counterpart [28]. For dark sirens, when adopting the spectral siren method, we only consider 42 BBH events; when adopting the dark siren method, we can consider all dark sirens and incorporate the  $K$ -band galaxies from

the extended galaxy list for the advanced detector era (GLADE+) [60]. We assume the  $K$ -band absolute magnitudes in GLADE+ follow the Schechter function [61].

*Gravitational wave population models.* Following Ref. [62], we consider three BBH mass distribution models: Power Law + Peak, Broken Power Law, and Truncated. Power Law + Peak and Broken Power Law models are simple and characterized by a single structure in the power law but still preferred by GWTC-3 data, though there is evidence for substructures in the BHs primary mass spectrum around  $\sim 10 M_\odot$  [63]. The Truncated model is the first phenomenological model, strongly disfavored by GWTC-3 data, but we consider it only for comparison. We assume a uniform distribution between  $1 M_\odot$  and  $3 M_\odot$  for the NS mass model. For NSBH, the black hole mass distribution is the same as the primary black hole in BBH, and the neutron star mass distribution is the same as that in BNS. We assume the binary formation rate follows the star formation rate and use a phenomenological model from Ref. [64] to describe the redshift distribution of GW sources. Following Ref. [62], we neglect the potential evolution of the BBH mass distribution with redshift and the selection effect of spin distribution, because the BBH mass distribution is expected to evolve at a level below current statistical uncertainties in GW data's redshift range [65, 66], and the inclusion of spin distribution will not vary the detection probability by more than a factor of 2 [67].

*Strong lensing data.* We only consider RXJ1131-1231 [68–70] in our analysis, as it is the only SGL system entirely within the redshift coverage of our GW data. Specifically, the spectroscopic redshifts of the lens and the source are  $z_d = 0.295$  [71] and  $z_s = 0.657$  [72]. Mass-sheet transform (MST) is a main source of systematic error in time-delay cosmology, as it preserves lensing observables but rescales the absolute time delay and the inferred  $H_0$  value. The H0LiCOW collaboration addressed MST by modeling the deflector mass density profile using either a power law or a component model with an NFW dark matter halo [73]. In contrast, the TDCOSMO collaboration employed hierarchical Bayesian analysis to break MST using only stellar kinematics [74]. We employ both the H0LiCOW and TDCOSMO methods and assess their impact on our results.

*Results and discussions.—Likelihood.* We constrain  $d(z)$  and  $H_0$  through the public Bayesian analysis code `Bilby` [75] and the Markov chain Monte Carlo sampler `emcee` [76] using GW data and SGLTD data. The logarithm of the total likelihood  $\mathcal{L}$  is given by

$$\ln(\mathcal{L}) = \ln(\mathcal{L}_{\text{SGL}}) + \ln(\mathcal{L}_{\text{GW}}), \quad (6)$$

where  $\mathcal{L}_{\text{SGL}}$  is the likelihood function of the SGLTD data. When using the H0LiCOW method to break MST, we obtain  $\mathcal{L}_{\text{SGL}}$  through kernel density estimation based on  $D_{\Delta t}$  and  $D_A(z_d)$  samples from Ref. [70]. When using the TDCOSMO method to break MST, we use the public

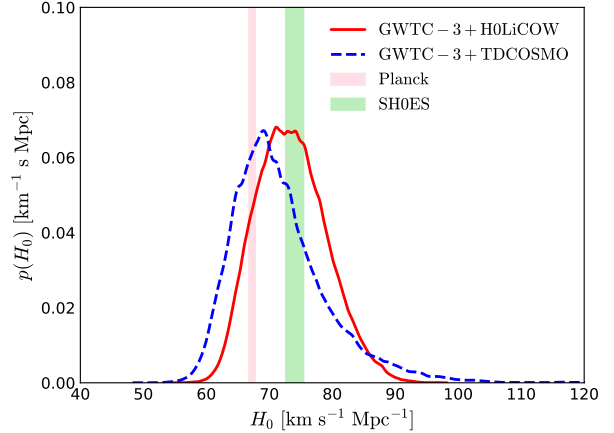


FIG. 1. Posterior distributions of  $H_0$  using 47 GW events and RXJ1131-1231 in the polynomial model. The red solid line and the blue dashed line represent the cases of using the H0LiCOW method and the TDCOSMO method to break MST, respectively. The pink and green shaded areas show the 68% confidence interval from the Planck 2018 CMB inference in the  $\Lambda$ CDM model and the SH0SE distance ladder measurement in the local universe, respectively.

code from Ref. [74] to obtain  $\mathcal{L}_{\text{SGL}}$ . In this case, we incorporate 33 lenses from the Sloan Lens ACS survey [77] to further constrain the deflector mass density profiles and jointly infer cosmological parameters and SGLTD model parameters.  $\mathcal{L}_{\text{GW}}$  is the likelihood function of the GW data. We use the public code `ICAROGW` [78] to calculate the hierarchical likelihood  $\mathcal{L}_{\text{GW}}$  of the GW data.

Following Refs. [22, 53], we model  $d(z)$  with a polynomial. By calculating the Bayesian information criterion for fitting GW data, we find that a third-order polynomial is sufficient to fit current GW data. We assume  $d(0) = 0$  and  $d'(0) = 1$ , so the third-order polynomial has two free parameters.

*Priors.* We take flat priors for all free parameters, with prior ranges specified as follows:  $H_0 \in [20, 140] \text{ km s}^{-1} \text{ Mpc}^{-1}$  and the  $i$ -order coefficient  $c_i \in [-1, 1]$  in polynomials. We also consider the case of using only SGLTD data, and we assume the  $\Lambda$ CDM model in this case with  $\Omega_m \in [0, 1]$ . The population model parameters of GW and SGLTD data in the hierarchical likelihood may degenerate with  $H_0$ , so they appear as free parameters, with prior ranges taken from Ref. [62] and Ref. [74], respectively. In this work, we obtain  $H_0$  constraint results assuming  $\Omega_K = 0$  in most cases. We also consider releasing  $\Omega_K$  as a free parameter with the prior range of  $\Omega_K \in [-2, 2]$  to analyze its impact on our results.

*Constraints on  $H_0$ .* We jointly constrain cosmological parameters and population model parameters of the GW and SGLTD data, with  $H_0$  constraint results summarized in Table I. We consider various combinations of observation data and model assumptions to comprehen-

TABLE I. Constraint values and precisions of  $H_0$  with various data choices, BBH mass distribution models, and MST treatment methods. The results in the first eight rows are cosmological-model-independent, while those in the last two rows are derived under the  $\Lambda$ CDM model.  $H_0$  is in the unit of  $\text{km s}^{-1} \text{Mpc}^{-1}$ , and  $\Delta H_0/H_0$  represents the precisions of  $H_0$  constraints at the 68% CL.

Data	BBH's mass model	MST treatment method	$H_0$ ( $\Delta H_0/H_0$ )	Condition
47 events + RXJ1131-1231	Power Law + Peak	H0LiCOW	$73.22_{-5.43}^{+5.95}$ (7.77%)	none
	Power Law + Peak	H0LiCOW	$76.26_{-7.34}^{+10.60}$ (11.76%)	unfix $\Omega_K$
	Power Law + Peak	TDCOSMO	$70.40_{-5.60}^{+8.03}$ (9.68%)	none
42 events + RXJ1131-1231	Power Law + Peak	H0LiCOW	$73.78_{-6.85}^{+6.48}$ (9.03%)	without GLADE+
	Broken Power Law	H0LiCOW	$74.60_{-6.95}^{+6.40}$ (8.95%)	without GLADE+
	Truncated	H0LiCOW	$74.89_{-6.17}^{+5.91}$ (8.07%)	without GLADE+
43 events + RXJ1131-1231	Power Law + Peak	H0LiCOW	$73.28_{-6.24}^{+6.16}$ (8.46%)	none
	Power Law + Peak	H0LiCOW	$73.27_{-5.64}^{+5.90}$ (7.87%)	without GLADE+
RXJ1131-1231	none	H0LiCOW	$77.33_{-3.30}^{+3.34}$ (4.29%)	$\Lambda$ CDM
	none	TDCOSMO	$68.65_{-7.01}^{+8.15}$ (4.29%)	$\Lambda$ CDM

sively analyze their impacts on our results.

We obtain our baseline result using 47 GW events combined with RXJ1131-1231, shown in the first row of Table I. In this case, we incorporate GLADE+ to obtain redshifts of GW dark sirens and employ mass model assumptions to break MST (the H0LiCOW method). We obtain  $H_0 = 73.22_{-5.43}^{+5.95} \text{ km s}^{-1} \text{ Mpc}^{-1}$  with a precision of 7.77%. Here and later, the constraint precision is of 68% confidence level (CL). This result is more consistent with the distance ladder measurement in the local universe and differs from the Planck TT, TE, EE+low E result [1] in the  $\Lambda$ CDM model by  $5.95 \text{ km s}^{-1} \text{ Mpc}^{-1}$ , with a deviation of about  $1\sigma$ .

Unfixing  $\Omega_K$  and using the same data and model assumptions as the baseline case, we obtain  $H_0 = 76.26_{-7.34}^{+10.60} \text{ km s}^{-1} \text{ Mpc}^{-1}$  with a precision of 11.76% and  $\Omega_K = 0.79_{-1.24}^{+0.83}$ , shown as in the second row of Table I. Compared with the baseline result, this result has a higher central value of  $H_0$  with a worse constraint precision on  $H_0$ . Compared with the analysis of Ref. [22] using SNe Ia and SGLTD data, we obtain the same deviation trend on the  $H_0$  central value after unfixing  $\Omega_K$ , because we find the same positive correlation between  $H_0$  and  $\Omega_K$ . Our  $\Omega_K$  result favors an open universe, which is consistent with other late-time cosmological probes [79] and differs from the Planck CMB result [1], but the deviation is less than  $1\sigma$  due to the poor constraint precision.

Applying the hierarchical inference approach to break MST (the TDCOSMO method), we obtain  $H_0 = 70.40_{-5.60}^{+8.03} \text{ km s}^{-1} \text{ Mpc}^{-1}$  with a precision of 9.68%,

shown as in the third row of Table I. Compared with the baseline result, this approach estimates a lower  $H_0$  central value and a worse constraint precision on  $H_0$ . See Fig. 1 for a visualization of the variation in  $H_0$  constraint results. To further investigate this deviation in the  $H_0$  central value and the worsening in constraint precision, we constrain  $H_0$  using SGLTD data alone in the  $\Lambda$ CDM model, with results presented in the last two rows of Table I. We can observe that the central value of  $H_0$  shows a similar bias but with an even bigger magnitude. The deviation in the central value of  $H_0$  from different methods of treating MST could be due to that we have only one SGLTD data point, which may possess huge statistical errors. Furthermore, the TDCOSMO method relies on kinematic measurements, where the choice of kinematic modeling and priors have a significant impact on cosmological inferences [80]. The worsening in the  $H_0$  constraint precisions of using the TDCOSMO method is predictable, as the hierarchical approach breaks MST using only kinematic information of the deflector galaxy, having a larger error budget, and the uncertainties fully propagate into the cosmological parameter inferences [74].

In GW data, obtaining redshifts for dark sirens relies on GW population models. Since BBH events are the majority of current GW data, their population model assumptions might impact results. To assess this, we constrain  $H_0$  using 42 BBHs and RXJ1131-1231, testing three BBH mass models: Power Law + Peak, Broken Power Law, and Truncated. Results are in the fourth

to sixth rows of Table I. To focus on the GW population model's impact, we exclude the GLADE+ catalog and use the spectral siren method to obtain redshifts of the 42 BBH events. We find that the estimated central values of  $H_0$  from three BBH mass models are nearly the same, different from the results using 42 BBHs alone in the  $w$ CDM model [62], especially when assuming the Truncated model. We obtain an improved  $H_0$  constraint precision when assuming the Truncated model, mainly because the Truncated model has fewer free model parameters.

The galaxy catalog and EM counterparts are two EM observations in GW data. To assess how incorporating GLADE+ affects our results, we constrain  $H_0$  using 42 BBH events and RXJ1131-1231, as shown in the seventh row of Table I. We find only a 0.57% improvement in the  $H_0$  constraint precision compared with the result using the same data and model assumptions but without GLADE+, shown in the fourth row of Table I, mainly because the completeness of GALDE+ in the  $K$  band decreases with increasing distance, reaching about 50% at around 420 Mpc [60]. Additionally, we find a  $\sim 40\%$  improvement in the  $H_0$  constraint precision compared with the result from GW170817 and its EM counterpart using the Hubble law. When we add GW170817 with its EM counterpart to 42 BBH events and RXJ1131-1231, we obtain a similar  $H_0$  constraint precision as the baseline result, as shown in the eighth row of Table I, showing that the bright siren provides the majority of cosmological constraints.

*Conclusions.*— The Hubble tension has emerged as a crisis in cosmology, and a late-time cosmological-model-independent determination of  $H_0$  can help resolve this problem. Using GW standard sirens to calibrate distances in SGLTDs can achieve cosmological-model-independent measurement for  $H_0$  in the FLRW metric through the distance-sum rule. Furthermore, GW standard sirens provide self-calibrated luminosity distance measurements and are more suitable for calibrating distances in SGLTDs than other distance indicators, such as SNe Ia and quasars. In this letter, we propose using GW dark sirens to extend the limited redshift range of the bright siren and, for the first time, use 47 GW events from GWTC-3 and the SGLTD data RXJ1131-1231 to measure  $H_0$  without assuming a specific cosmological model.

Fixing  $\Omega_K = 0$  and breaking MST through the mass model assumption of the deflector galaxy, we obtain  $H_0 = 73.22^{+5.95}_{-5.43}$  km s $^{-1}$  Mpc $^{-1}$ , with a 7.77% precision. This result deviates around  $1\sigma$  from the Planck 2018 CMB results in the  $\Lambda$ CDM model. If using the hierarchical inference to break MST with kinematic measurements, we obtain  $H_0 = 70.40^{+8.03}_{-5.60}$  km s $^{-1}$  Mpc $^{-1}$  km s $^{-1}$  Mpc $^{-1}$ , with a 9.68% precision. When unfixing  $\Omega_K$ , we obtain  $H_0 = 76.26^{+10.60}_{-7.34}$  km s $^{-1}$  Mpc $^{-1}$ ,

with a 11.76% precision, and  $\Omega_K = 0.79^{+0.83}_{-1.24}$  by using the model assumption to break MST. Here,  $H_0$ 's central value rises due to its positive correlation with  $\Omega_K$ , and the  $\Omega_K$  result favors an open universe.

We find that the method of breaking MST influences our results, mainly because the SGLTD data plays a dominant role, and due to the limitation of GW data's redshifts, we only have one SGLTD data, which has huge statistical errors. We find that after combining with the SGLTD data, the choices on GW population models become less significant compared with using GW dark sirens alone. The GLADE+ catalog's impact is minor due to its high incompleteness. In contrast, adding GW170817 with its EM counterpart can significantly improve the constraint precision of  $H_0$  nearly without changing the estimated central value.

Since detecting more GW bright sirens is very difficult, it is crucial to further develop the cosmological applications of GW dark sirens. Remarkably, we find that the  $H_0$  constraint precision from 42 BBH events combined with RXJ1131-1231 is better than that measured using GW170817 through the Hubble law [26] by about 40%. This suggests that in the future, by increasing GW dark sirens' redshifts and including more SGLTDs, we can effectively reduce statistical errors of the single SGLTD data and achieve precise, model-independent measurement for  $H_0$  using only GW dark sirens and SGLTDs.

*Acknowledgments.* We are grateful to Ji-Guo Zhang, Guo-Hong Du, and Xianzhe TZ Tang for fruitful discussions. This work was supported by the National SKA Program of China (Grants Nos. 2022SKA0110200 and 2022SKA0110203), the National Natural Science Foundation of China (Grants Nos. 12473001, 11975072, 11835009, and 11875102), and the National 111 Project (Grant No. B16009).

---

\* qijingzhao@mail.neu.edu.cn

† zhangxin@mail.neu.edu.cn

- [1] N. Aghanim *et al.* (Planck), *Astron. Astrophys.* **641**, A6 (2020), [Erratum: *Astron. Astrophys.* 652, C4 (2021)], arXiv:1807.06209 [astro-ph.CO].
- [2] A. G. Riess *et al.*, *Astrophys. J. Lett.* **934**, L7 (2022), arXiv:2112.04510 [astro-ph.CO].
- [3] R.-Y. Guo, J.-F. Zhang, and X. Zhang, *JCAP* **02**, 054 (2019), arXiv:1809.02340 [astro-ph.CO].
- [4] G. D'Amico, L. Senatore, P. Zhang, and H. Zheng, *JCAP* **05**, 072 (2021), arXiv:2006.12420 [astro-ph.CO].
- [5] J. C. Hill, E. McDonough, M. W. Toomey, and S. Alexander, *Phys. Rev. D* **102**, 043507 (2020), arXiv:2003.07355 [astro-ph.CO].
- [6] N. Aghanim *et al.* (Planck), *Astron. Astrophys.* **607**, A95 (2017), arXiv:1608.02487 [astro-ph.CO].
- [7] D. O. Jones *et al.*, *Astrophys. J.* **867**, 108 (2018), arXiv:1805.05911 [astro-ph.CO].
- [8] W. D. Kenworthy, D. Scolnic, and A. Riess, *Astrophys.*

- J. **875**, 145 (2019), arXiv:1901.08681 [astro-ph.CO].
- [9] A. G. Riess, S. Casertano, W. Yuan, L. M. Macri, and D. Scolnic, *Astrophys. J.* **876**, 85 (2019), arXiv:1903.07603 [astro-ph.CO].
- [10] Y. Akrami *et al.* (Planck), *Astron. Astrophys.* **641**, A7 (2020), arXiv:1906.02552 [astro-ph.CO].
- [11] A. G. Riess *et al.*, *Astrophys. J.* **977**, 120 (2024), arXiv:2408.11770 [astro-ph.CO].
- [12] S. Li, G. S. Anand, A. G. Riess, S. Casertano, W. Yuan, L. Breuval, L. M. Macri, D. Scolnic, R. Beaton, and R. I. Anderson, *Astrophys. J.* **976**, 177 (2024), arXiv:2408.00065 [astro-ph.CO].
- [13] M. Pascale *et al.*, *Astrophys. J.* **979**, 13 (2025), arXiv:2403.18902 [astro-ph.CO].
- [14] S. Li, A. G. Riess, S. Casertano, G. S. Anand, D. M. Scolnic, W. Yuan, L. Breuval, and C. D. Huang, *Astrophys. J.* **966**, 20 (2024), arXiv:2401.04777 [astro-ph.CO].
- [15] A. G. Riess, G. S. Anand, W. Yuan, S. Casertano, A. Dolphin, L. M. Macri, L. Breuval, D. Scolnic, M. Perrin, and I. R. Anderson, *Astrophys. J. Lett.* **962**, L17 (2024), arXiv:2401.04773 [astro-ph.CO].
- [16] W. L. Freedman, B. F. Madore, I. S. Jang, T. J. Hoyt, A. J. Lee, and K. A. Owens, (2024), arXiv:2408.06153 [astro-ph.CO].
- [17] A. J. Lee, W. L. Freedman, B. F. Madore, I. S. Jang, K. A. Owens, and T. J. Hoyt, (2024), arXiv:2408.03474 [astro-ph.GA].
- [18] L. Huang, S.-J. Wang, and W.-W. Yu, *Sci. China Phys. Mech. Astron.* **68**, 220413 (2025), arXiv:2401.14170 [astro-ph.CO].
- [19] L. Huang, R.-G. Cai, S.-J. Wang, J.-Q. Liu, and Y.-H. Yao, (2024), arXiv:2410.06053 [astro-ph.CO].
- [20] L. Perivolaropoulos, *Phys. Rev. D* **110**, 123518 (2024), arXiv:2408.11031 [astro-ph.CO].
- [21] S. Räsänen, K. Bolejko, and A. Finoguenov, *Phys. Rev. Lett.* **115**, 101301 (2015), arXiv:1412.4976 [astro-ph.CO].
- [22] T. Collett, F. Montanari, and S. Rasanan, *Phys. Rev. Lett.* **123**, 231101 (2019), arXiv:1905.09781 [astro-ph.CO].
- [23] J.-J. Wei and F. Melia, *Astrophys. J.* **897**, 127 (2020), arXiv:2005.10422 [astro-ph.CO].
- [24] J.-Z. Qi, Y. Cui, W.-H. Hu, J.-F. Zhang, J.-L. Cui, and X. Zhang, *Phys. Rev. D* **106**, 023520 (2022), arXiv:2202.01396 [astro-ph.CO].
- [25] B. F. Schutz, *Nature* **323**, 310 (1986).
- [26] B. P. Abbott *et al.* (LIGO Scientific, Virgo, 1M2H, Dark Energy Camera GW-E, DES, DLT40, Las Cumbres Observatory, VINROUGE, MASTER), *Nature* **551**, 85 (2017), arXiv:1710.05835 [astro-ph.CO].
- [27] B. P. Abbott *et al.* (LIGO Scientific, Virgo), *Phys. Rev. Lett.* **119**, 161101 (2017), arXiv:1710.05832 [gr-qc].
- [28] B. P. Abbott *et al.* (LIGO Scientific, Virgo, Fermi-GBM, INTEGRAL), *Astrophys. J. Lett.* **848**, L13 (2017), arXiv:1710.05834 [astro-ph.HE].
- [29] N. Dalal, D. E. Holz, S. A. Hughes, and B. Jain, *Phys. Rev. D* **74**, 063006 (2006), arXiv:astro-ph/0601275.
- [30] C. Cutler and D. E. Holz, *Phys. Rev. D* **80**, 104009 (2009), arXiv:0906.3752 [astro-ph.CO].
- [31] W. Zhao, C. Van Den Broeck, D. Baskaran, and T. G. F. Li, *Phys. Rev. D* **83**, 023005 (2011), arXiv:1009.0206 [astro-ph.CO].
- [32] R.-G. Cai and T. Yang, *Phys. Rev. D* **95**, 044024 (2017), arXiv:1608.08008 [astro-ph.CO].
- [33] R.-G. Cai, T.-B. Liu, X.-W. Liu, S.-J. Wang, and T. Yang, *Phys. Rev. D* **97**, 103005 (2018), arXiv:1712.00952 [astro-ph.CO].
- [34] L.-F. Wang, X.-N. Zhang, J.-F. Zhang, and X. Zhang, *Phys. Lett. B* **782**, 87 (2018), arXiv:1802.04720 [astro-ph.CO].
- [35] X.-N. Zhang, L.-F. Wang, J.-F. Zhang, and X. Zhang, *Phys. Rev. D* **99**, 063510 (2019), arXiv:1804.08379 [astro-ph.CO].
- [36] X. Zhang, *Sci. China Phys. Mech. Astron.* **62**, 110431 (2019), arXiv:1905.11122 [astro-ph.CO].
- [37] L.-F. Wang, Z.-W. Zhao, J.-F. Zhang, and X. Zhang, *JCAP* **11**, 012 (2020), arXiv:1907.01838 [astro-ph.CO].
- [38] Z.-W. Zhao, L.-F. Wang, J.-F. Zhang, and X. Zhang, *Sci. Bull.* **65**, 1340 (2020), arXiv:1912.11629 [astro-ph.CO].
- [39] J.-F. Zhang, M. Zhang, S.-J. Jin, J.-Z. Qi, and X. Zhang, *JCAP* **09**, 068 (2019), arXiv:1907.03238 [astro-ph.CO].
- [40] S.-J. Jin, D.-Z. He, Y. Xu, J.-F. Zhang, and X. Zhang, *JCAP* **03**, 051 (2020), arXiv:2001.05393 [astro-ph.CO].
- [41] L.-F. Wang, S.-J. Jin, J.-F. Zhang, and X. Zhang, *Sci. China Phys. Mech. Astron.* **65**, 210411 (2022), arXiv:2101.11882 [gr-qc].
- [42] H.-Y. Chen, M. Fishbach, and D. E. Holz, *Nature* **562**, 545 (2018), arXiv:1712.06531 [astro-ph.CO].
- [43] R. Gray *et al.*, *Phys. Rev. D* **101**, 122001 (2020), arXiv:1908.06050 [gr-qc].
- [44] L.-G. Zhu, Y.-M. Hu, H.-T. Wang, J.-d. Zhang, X.-D. Li, M. Hendry, and J. Mei, *Phys. Rev. Res.* **4**, 013247 (2022), arXiv:2104.11956 [astro-ph.CO].
- [45] L.-G. Zhu, L.-H. Xie, Y.-M. Hu, S. Liu, E.-K. Li, N. R. Napolitano, B.-T. Tang, J.-d. Zhang, and J. Mei, *Sci. China Phys. Mech. Astron.* **65**, 259811 (2022), arXiv:2110.05224 [astro-ph.CO].
- [46] J.-Y. Song, L.-F. Wang, Y. Li, Z.-W. Zhao, J.-F. Zhang, W. Zhao, and X. Zhang, *Sci. China Phys. Mech. Astron.* **67**, 230411 (2024), arXiv:2212.00531 [astro-ph.CO].
- [47] S.-J. Jin, Y.-Z. Zhang, J.-Y. Song, J.-F. Zhang, and X. Zhang, *Sci. China Phys. Mech. Astron.* **67**, 220412 (2024), arXiv:2305.19714 [astro-ph.CO].
- [48] S.-J. Jin, R.-Q. Zhu, J.-Y. Song, T. Han, J.-F. Zhang, and X. Zhang, *JCAP* **08**, 050 (2024), arXiv:2309.11900 [astro-ph.CO].
- [49] N. Muttoni, D. Laghi, N. Tamanini, S. Marsat, and D. Izquierdo-Villalba, *Phys. Rev. D* **108**, 043543 (2023), arXiv:2303.10693 [astro-ph.CO].
- [50] Y.-Y. Dong, J.-Y. Song, S.-J. Jin, J.-F. Zhang, and X. Zhang, (2024), arXiv:2404.18188 [astro-ph.CO].
- [51] S.-R. Xiao, Y. Shao, L.-F. Wang, J.-Y. Song, L. Feng, J.-F. Zhang, and X. Zhang, (2024), arXiv:2408.00609 [astro-ph.CO].
- [52] L.-G. Zhu, H.-M. Fan, X. Chen, Y.-M. Hu, and J.-d. Zhang, *Astrophys. J. Suppl.* **273**, 24 (2024), arXiv:2403.04950 [astro-ph.CO].
- [53] M.-D. Cao, J. Zheng, J.-Z. Qi, X. Zhang, and Z.-H. Zhu, *Astrophys. J.* **934**, 108 (2022), arXiv:2112.14564 [astro-ph.CO].
- [54] S. Refsdal, *Mon. Not. Roy. Astron. Soc.* **128**, 307 (1964).
- [55] S. H. Suyu, P. J. Marshall, M. W. Auger, S. Hilbert, R. D. Blandford, L. V. E. Koopmans, C. D. Fassnacht, and T. Treu, *Astrophys. J.* **711**, 201 (2010), arXiv:0910.2773 [astro-ph.CO].
- [56] S. R. Taylor, J. R. Gair, and I. Mandel, *Phys. Rev. D* **85**, 023535 (2012), arXiv:1108.5161 [gr-qc].
- [57] J. M. Ezquiaga and D. E. Holz, *Phys. Rev. Lett.* **129**, 061102 (2022), arXiv:2202.08240 [astro-ph.CO].

- [58] S. Mastrogiiovanni, D. Laghi, R. Gray, G. C. Santoro, A. Ghosh, C. Karathanasis, K. Leyde, D. A. Steer, S. Perriès, and G. Pierra, *Phys. Rev. D* **108**, 042002 (2023), arXiv:2305.10488 [astro-ph.CO].
- [59] R. Gray *et al.*, *JCAP* **12**, 023 (2023), arXiv:2308.02281 [astro-ph.CO].
- [60] G. Dálya *et al.*, *Mon. Not. Roy. Astron. Soc.* **514**, 1403 (2022), arXiv:2110.06184 [astro-ph.CO].
- [61] C. S. Kochanek, M. A. Pahre, E. E. Falco, J. P. Huchra, J. Mader, T. H. Jarrett, T. Chester, R. Cutri, and S. E. Schneider, *Astrophys. J.* **560**, 566 (2001), arXiv:astro-ph/0011456.
- [62] R. Abbott *et al.* (LIGO Scientific, Virgo, KAGRA), *Astrophys. J.* **949**, 76 (2023), arXiv:2111.03604 [astro-ph.CO].
- [63] R. Abbott *et al.* (KAGRA, VIRGO, LIGO Scientific), *Phys. Rev. X* **13**, 011048 (2023), arXiv:2111.03634 [astro-ph.HE].
- [64] P. Madau and M. Dickinson, *Ann. Rev. Astron. Astrophys.* **52**, 415 (2014), arXiv:1403.0007 [astro-ph.CO].
- [65] M. Fishbach and V. Kalogera, *Astrophys. J. Lett.* **914**, L30 (2021), arXiv:2105.06491 [astro-ph.HE].
- [66] L. A. C. van Son, S. E. de Mink, T. Callister, S. Justham, M. Renzo, T. Wagg, F. S. Broekgaarden, F. Kummer, R. Pakmor, and I. Mandel, *Astrophys. J.* **931**, 17 (2022), arXiv:2110.01634 [astro-ph.HE].
- [67] K. K. Y. Ng, S. Vitale, A. Zimmerman, K. Chatzioannou, D. Gerosa, and C.-J. Haster, *Phys. Rev. D* **98**, 083007 (2018), arXiv:1805.03046 [gr-qc].
- [68] S. H. Suyu *et al.*, *Astrophys. J.* **766**, 70 (2013), arXiv:1208.6010 [astro-ph.CO].
- [69] S. H. Suyu *et al.*, *Astrophys. J. Lett.* **788**, L35 (2014), arXiv:1306.4732 [astro-ph.CO].
- [70] G. C. F. Chen *et al.* (H0LiCOW), *Mon. Not. Roy. Astron. Soc.* **490**, 1743 (2019), arXiv:1907.02533 [astro-ph.CO].
- [71] D. Sluse, J. Surdej, J. F. Claeskens, D. Hutsemekers, C. Jean, F. Courbin, T. Nakos, M. Billeres, and S. V. Khmil, *Astron. Astrophys.* **406**, L43 (2003), arXiv:astro-ph/0307345.
- [72] D. Sluse, J. F. Claeskens, D. Hutsemekers, and J. Surdej, *Astron. Astrophys.* **468**, 885 (2007), arXiv:astro-ph/0703030.
- [73] J. F. Navarro, C. S. Frenk, and S. D. M. White, *Astrophys. J.* **490**, 493 (1997), arXiv:astro-ph/9611107.
- [74] S. Birrer *et al.*, *Astron. Astrophys.* **643**, A165 (2020), arXiv:2007.02941 [astro-ph.CO].
- [75] G. Ashton *et al.*, *Astrophys. J. Suppl.* **241**, 27 (2019), arXiv:1811.02042 [astro-ph.IM].
- [76] D. Foreman-Mackey, D. W. Hogg, D. Lang, and J. Goodman, *Publ. Astron. Soc. Pac.* **125**, 306 (2013), arXiv:1202.3665 [astro-ph.IM].
- [77] A. S. Bolton, S. Burles, L. V. E. Koopmans, T. Treu, and L. A. Moustakas, *Astrophys. J.* **638**, 703 (2006), arXiv:astro-ph/0511453.
- [78] S. Mastrogiiovanni, G. Pierra, S. Perriès, D. Laghi, G. Caneva Santoro, A. Ghosh, R. Gray, C. Karathanasis, and K. Leyde, *Astron. Astrophys.* **682**, A167 (2024), arXiv:2305.17973 [astro-ph.CO].
- [79] P.-J. Wu and X. Zhang, (2024), arXiv:2411.06356 [astro-ph.CO].
- [80] S. Birrer, A. Amara, and A. Refregier, *JCAP* **08**, 020 (2016), arXiv:1511.03662 [astro-ph.CO].